Journal of Science and Technology in Civil Engineering, HUCE (NUCE), 2023, 17 (1): 111–124

A STUDY ON THE PROBABILISTIC SAFETY ASSESSMENT OF THE TRUSS STRUCTURE DESIGNED BY THE LRFD CODE

Nhu Son Doan[a,*]

[a] *Faculty of Civil Engineering, Vietnam Maritime University, 484 Lach Tray street, Le Chan district, Haiphong*

Article history:
Received 12/12/2022, Revised 11/01/2023, Accepted 16/01/2023

Abstract

The probabilistic analyses provide a more rational approach for the safety assessment of structures since they consider the uncertainties in the calculations. Consequently, the design specifications of engineering structures are gradually transformed from the allowable stress design to the reliability-based specifications such as load and resistance factors design (LRFD) or partial safety factor design. The partial safety factors and the load and resistance factors provided in the reliability-based design codes are successfully determined from probabilistic frameworks. However, these specifications are classified into semi-probabilistic-based codes because no probabilistic analysis is required in the design practice. Thus, the actual reliability index of the design solutions may not be as close to the target value as expected. This study employs the fully probabilistic analysis as an additional analysis to examine the reliability index of an LRFD-based design of the truss structure. A planar truss, which is designed following the semi-probabilistic code, is thoroughly examined. Several feasible sections are first designed using the LRFD code. Then, the actual reliability indexes of truss structures are evaluated to check if they meet the target reliability index specified in the reliability-based design codes. The tension and compression members concerning the strength limit state and the maximum deflection presenting for serviceability are investigated as representative performances. The results of the probabilistic analyses indicate that the reliability indexes for the strength limit state are higher than the target value stipulated in the LRFD code. Compared to the tension members, more redundancy in terms of reliability index is observed for compression elements, although they are both designed at the limit state. Moreover, the reliability index obtained for the serviceability limit state is strongly dependent on the component (i.e., floor or roof) where the truss is utilized.

Keywords: reliability analysis; fully probabilistic analysis; Monte-Carlo simulation; truss structure; LRFD.

https://doi.org/10.31814/stce.nuce2023-17(1)-09

1. Introduction

The probabilistic analyses appear to be efficient and rational methods for assessing safety structures considering uncertainties [1–3]. Particularly, the uncertainties that are inherently involved in the operation loads or the strength properties of materials built in the structures are considered in the probabilistic analysis. This feature set the foundation for probabilistic-based design specifications such as the partial safety method or load and resistance factor design (LRFD) [4, 5]. The uncertainties in load and resistance components are examined and considered during the calibration of the factors specified in the design codes. Moreover, the applications of the probabilistic-based design codes are also

[*]Corresponding author. *E-mail address:* vanson.ctt@vimaru.edu.vn (Doan, N. S.)

similar to those of the allowable stress design. These two features make the probabilistic-based design codes more efficient and widely applied. Particularly, the applications of the probabilistic-based design codes intend to provide a uniform and consistent design class. However, these probabilistic-based design codes above mentioned are identified as semi-probabilistic analyses since no risk analysis is performed during the design phase [6, 7]. That means the probabilistic quantities such as the reliability index (RI) or probability of failure are not determined for the designed solutions. Therefore, the satisfaction in terms of probabilistic quantities becomes questionable [8].

The MVFOSM (mean value first-order second-moment method) or FORM (first-order reliability method) were prevailingly conducted to determine the resistance factors in most of the reliability-based codes. For example, MVFOSM was applied to evaluate the resistance factors in some American specifications, such as AASHTO 2017 [6] or AISC 360-16 [7]. Alternatively, FORM was performed during the development of the design code of the harbor facilities in Japan [9]. However, it was reported that the MVFOSM and FORM could not produce good results if the performance function is highly nonlinear or when the input variables have high variations [3, 5]. That means the use of the resistance factors recommended in the above specifications may not result in solutions that have the RIs close enough to the target values. Contrastingly, Monte-Carlo simulation (MCS) - a fully probabilistic approach [3, 10], which does not require any assumption on the distribution properties of the performance functions is reported as the most accurate method. Thus, MCS is utilized in this work for validation purposes.

Recently, probabilistic analyses have been recommended to be performed to check if the actual RIs of the designed solutions meet the target values specified in the reliability-based codes. Several studies indicated that the actual RI is not always as close to the targets as expected. Some reasons were indicated, such as the differences between the wide uncertainty range of site conditions and the applied range of testing methods, or the different transformations utilized [11, 12]. The additional reliability analysis aims to provide rational insights into the design solutions. In addition, the reliability calculations help to compare different design solutions which are designed following the same specifications. Based on that the most suitable solution can be identified.

Based on the discussions above, this study applies the fully probabilistic analysis to investigate the probabilistic results of the truss structures designed using LRFD code. Namely, the MCS is combined with the finite element method (FEM) to evaluate the failure probability of the truss structure. For this purpose, based on MATLAB [13], a MATLAB program was first developed for FEM-based analysis of truss structures. Then, the MCS technique is adopted to generate the sampling set of the uncertain input variable. The data from MCS are then driven into the MATLAB program to evaluate the performance functions. The strength limit states concerning tension and compression behaviors of the truss members, and the deflection representing the serviceability limit state are thoroughly examined.

2. Deterministic analysis and LRFD-based design of truss members

FEMs were widely utilized in most engineering problems, and their applications to structural problems were well presented in many studies [14, 15]. Several important steps are summarized in Fig. 1. A MATLAB program (*FEM-Truss*) is developed following Fig. 1 for analyzing truss problems. A truss structure shown in Fig. 2(a), adapted from Blum [16] and Packer et al. [17], is used to validate the developed MATLAB program. The i^{th} nominal (unfactored) dead load, D_i is 18 kN; and the i^{th} nominal live load, L_i is 54kN ($i = 1 - 7$) [16]. The resultants of axial forces are calculated for the load combination of 1.2D + 1.6L [18] and reported in Fig. 2(b). The maximum tension load of 1215 kN, and the most critical compression load of 1147kN are determined. The results obtained from the program are identical to those reported in the two previous studies [16, 17]. This comparison confirms the accuracy of the MATLAB program.

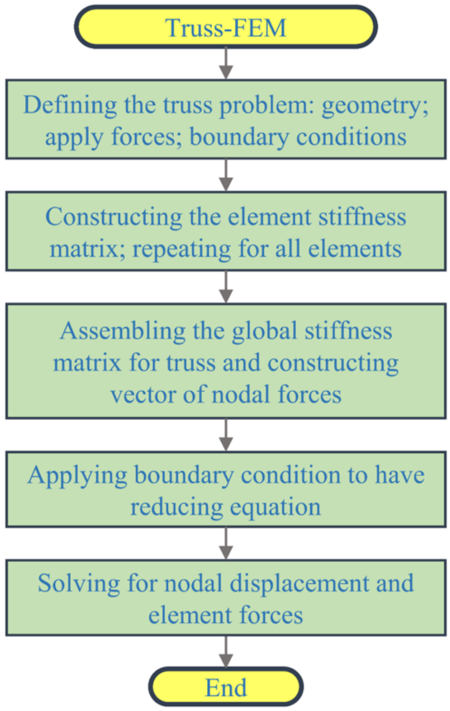

Figure 1. Flowchart for FEM-based analysis of truss structures

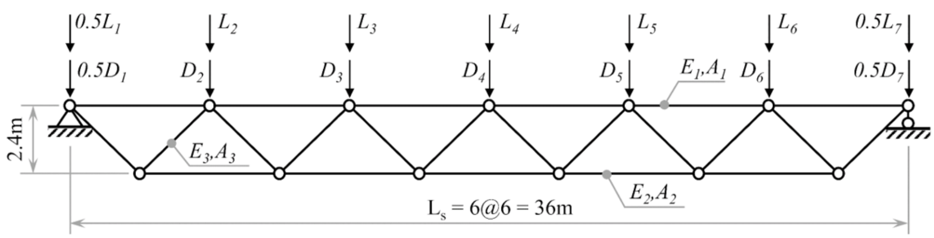

(a) Truss profile

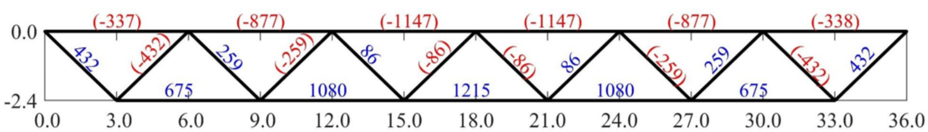

(b) Resultant axial forces obtained from load combination of 1.2D+1.6L

Figure 2. Example of Warren truss

The sections of the truss members are then designed following the Specification for Structural Steel Building of American Institute of Steel Construction (AISC 360-16) [7]. The truss bars are classified into three different groups for simplicity, i.e., tension bars in the lower chord; compression bars in the upper chord; and web bars. Noticeably, AISC 360-16 provides both ASD (Allowable Strength Design) and LRFD approaches to designing steel structures. This study focuses on the LRFD approach to designing element sections. The sections of truss members were provided in Packer [17] and adapted in Blum [16]. However, the two previous studies used the same sections for the tension and the compression members. On the contrary, this study investigates the probabilistic results when using different sections, and only sections of the web members are kept as 120 × 120 × 4 mm of square hollow section (SHS) following Blum [16]. Then, the tension bars are designed following Chapter D, and the compression bars are designed based on Chapter E of AISC 360-16. Finally, the vertical deflection is checked with the specified value of $L_s/360$ (i.e., 10 cm) assuming for floor members (where L_s is the span length of the truss).

The typical sections of the cold-formed SHS of SSAB (Svenska Aeroplan Aktie Bolag) Domex Tube (provided on www.ssab.com for steel sections) are chosen for the design process in this study. The yield strength of 350 kPa and Young's modulus of 200 GPa are utilized for the steel material. The strength of tension and compression elements are then verified following AISC 360-16 with the most critical axial forces reported in Fig. 2(b). The procedure for checking tension and compression members is briefly summarized in Fig. 3. The width of the SHS sections is chosen from 120 mm to 220 mm for the chord members. Notably, the same resistance factors of 0.9 (i.e., ϕ_t, ϕ_c) specified in AISC 360-16 are used for designing both tension and compression members.

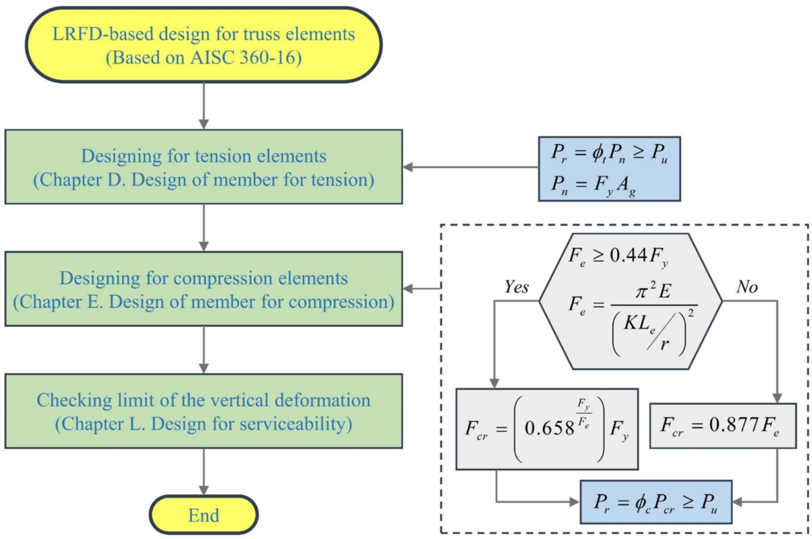

Figure 3. Strength checking for tension and compression members

In Fig. 3, P_u is the axial force in the truss bars. P_r and P_n correspond to the factored and nominal resistances. F_y, E, A_g are yield strength, Elastic modulus, and cross-section area, respectively. The critical stress (F_{cr}) in compression bars is determined based on the elastic buckling stress (F_e), the effective length factor (K), and the element length (L_e). The results computed from all considered sections are summarized in Fig. 4 for tension bars and Fig. 5 for compression bars. The circle markers and the associated numbers in the figures indicate reasonable sections, which are within 5% of redundancy. It is seen that there are three suitable sections for tension bars (120 × 120 × 10 mm; 140 × 140 × 8 mm; and 150 × 150 × 7.1 mm); and three feasible sections for compression bars (180 × 180 ×

8.8 mm; 200 × 200 × 7.1 mm; and 220 × 220 × 6.0 mm). Here, it is worth noting that the sections for compression bars are much bigger than those for tension members, although the compression force is smaller than the tension force.

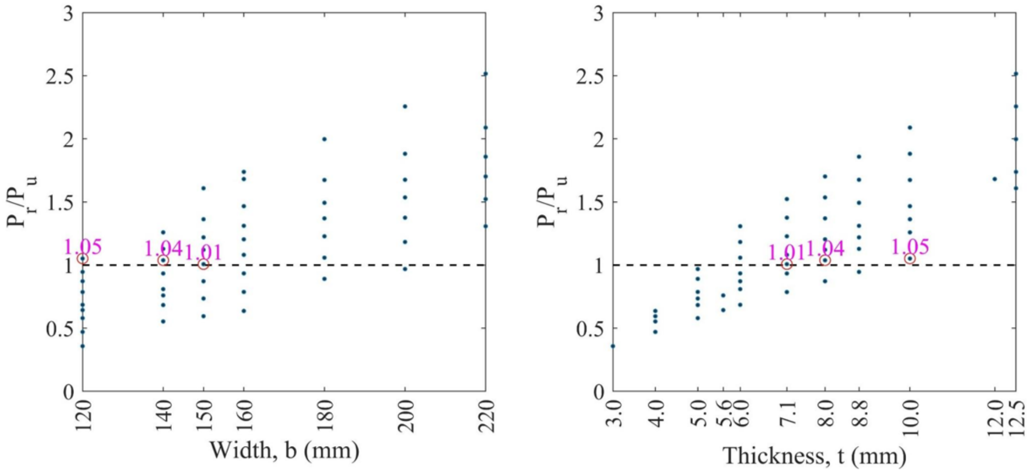

Figure 4. Strength checking for tension members

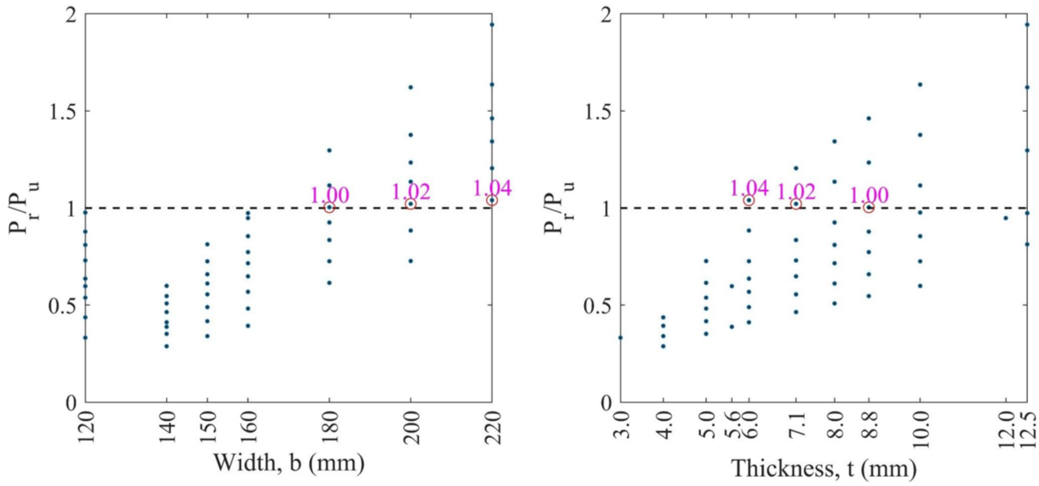

Figure 5. Strength checking for compression members

The chosen sections, which have the ratio between P_r and P_u close to unity aim to achieve the LRFD limit state. The LRFD limit state implies that the RI of the structure is expected to be close to the target value. Then, the slenderness ratio limitation (300 for tension bars and 200 for compression bars) is determined based on the effective length of the components. The effective length factor (K) of 0.9 is selected for the compression bars [16, 17]. The slenderness ratios are shown in Fig. 6 for all SHS sections of SSAB considered in this study. Moreover, the limiting width-thickness ratios for compression elements are checked to desire the compact sections, i.e., protecting local buckling (Table 4.1 of AISC 360-16 [7]). The summarizations are illustrated in Fig. 7.

Based on the buckling conditions, it is seen that all sections satisfy the global buckling condition (Fig. 6). However, the 220 × 220 × 6 mm section is not desired for local buckling checks (Fig. 7).

Thus, two sections for compression and three sections for tension bars (among the six sections above mentioned) are suitable for the probabilistic analysis.

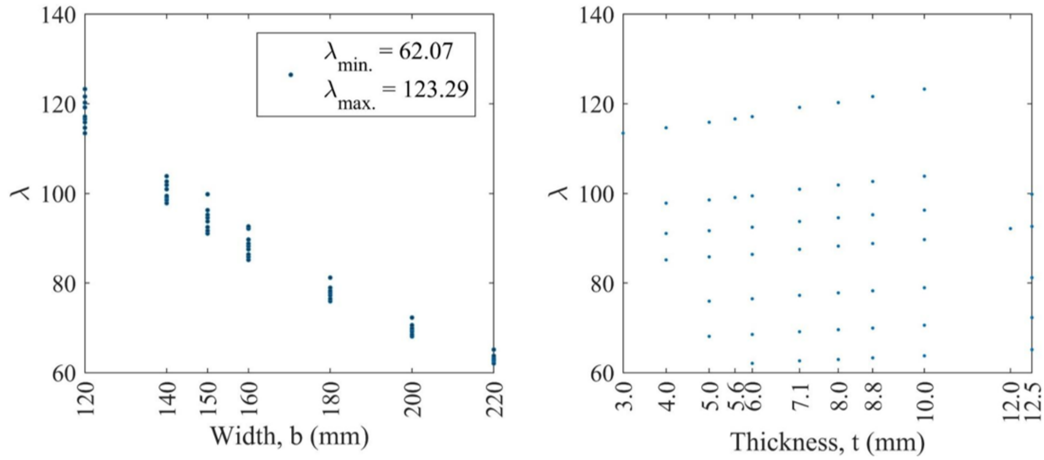

Figure 6. Global buckling of chord bars ($\lambda = KL_s/r$)

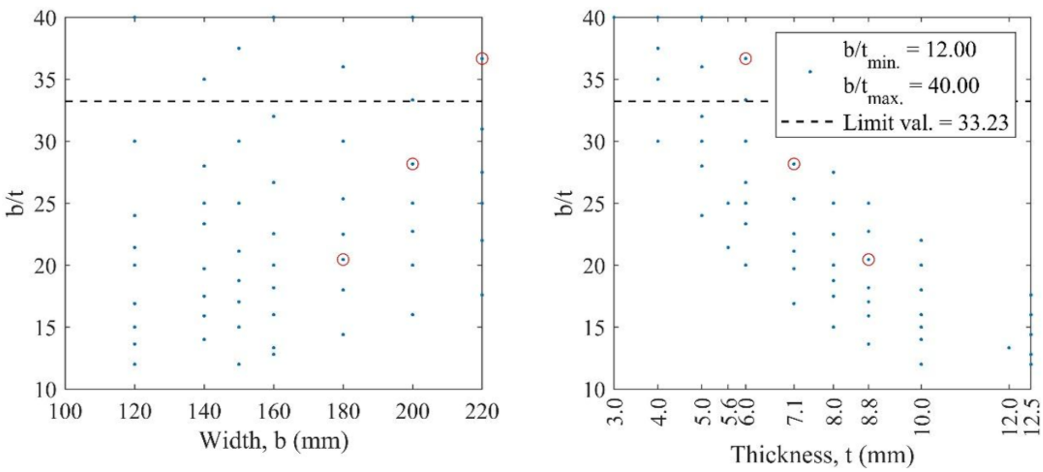

Figure 7. Local buckling limitation of compression sections

3. Fully probabilistic analysis for truss structure

The reliability analysis methods have been presented in the literature [3, 19]. Three different reliability analysis methods were applied to evaluate the overall stability of vertical breakwaters [10]. It was proven that the Monte Carlo simulation is a straightforward and robust approach to probabilistic analysis. The MCS provides not only the failure probability but also the statistical information on the performance functions. Moreover, MCS is the most suitable approach for nonlinear and high-dimension problems. Therefore, MCS is stated to be superior to the point estimate methods. The most critical disadvantage of MCS is the computing time and effort required since a huge number of calculations is needed [20]. However, the integration of the MCS with FEM has been more convenient with the aid of the computer recently. The conjunction of the FEM with MCS is presented in Fig. 8.

The truss problem is defined in the first step, in which the truss profile, applied load, and boundary conditions are provided. The uncertainties considered in the truss problem are also defined in this step. In this work, the truss profile and boundary conditions are treated deterministically. The uncertainty variables are referred from previous studies [16, 21–23] relating to AISC 360-16 and summarized in Table 1. It is seen in the table that the first five random variables are from steel sections and material properties. Meanwhile, the last two random variables are taken from excitation loads. The COV defined in the table is the coefficient of variation, which is the ratio between the standard deviation and the mean value μ. μ is the mean of the bias factors that is defined as the ratio between the mean and the nominal values [4].

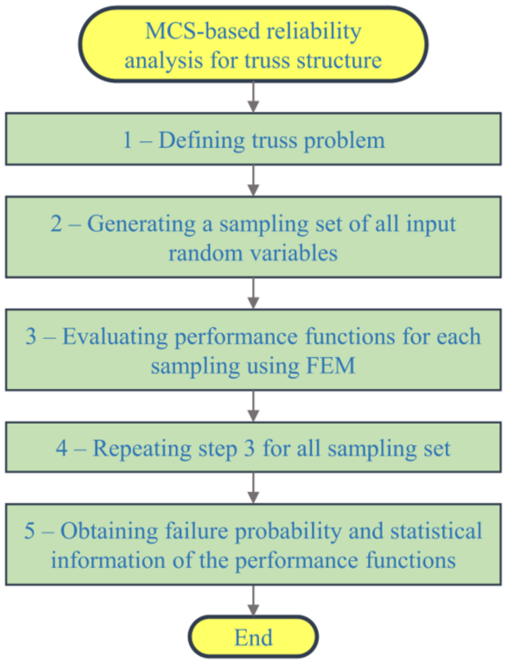

Figure 8. Integration of MCS and FEM for reliability analysis of truss structures

Table 1. Random variables considered

No.	Symbol	Description	Nominal	μ	COV	Distribution
1	t_c	Thickness of comp. bars	7.1 or 8.8 mm	0.964	0.04	Normal
2	t_t	Thickness of tension bars	7.1; 8.0; 10.0 mm	0.964	0.04	Normal
3	t_w	Thickness of web members	4.0 mm	0.964	0.04	Normal
4	E	Young's modulus	200 GPa	1.00	0.06	Normal
5	F_y	Yield strength	350 MPa	1.10	0.10	Normal
6	D	Dead load	18 kN	1.05	0.10	Normal
7	L	Live load	54 kN	1.00	0.25	Extreme type 1

In Step 2, MCS is performed to generate a sampling set of all random input variables using the statistics defined in the first step. The size of the MCS (N_{MCS}), which strongly influences the calculation performance, is recommended in previous studies [3, 20]. In this study, the size of MCS is chosen as 1 million so that the COV of the failure probability is not higher than 0.18 (assuming the RI is about 4.0). The histograms of Young's modulus, yield strength, dead load, and live load are illustrated in Fig. 9.

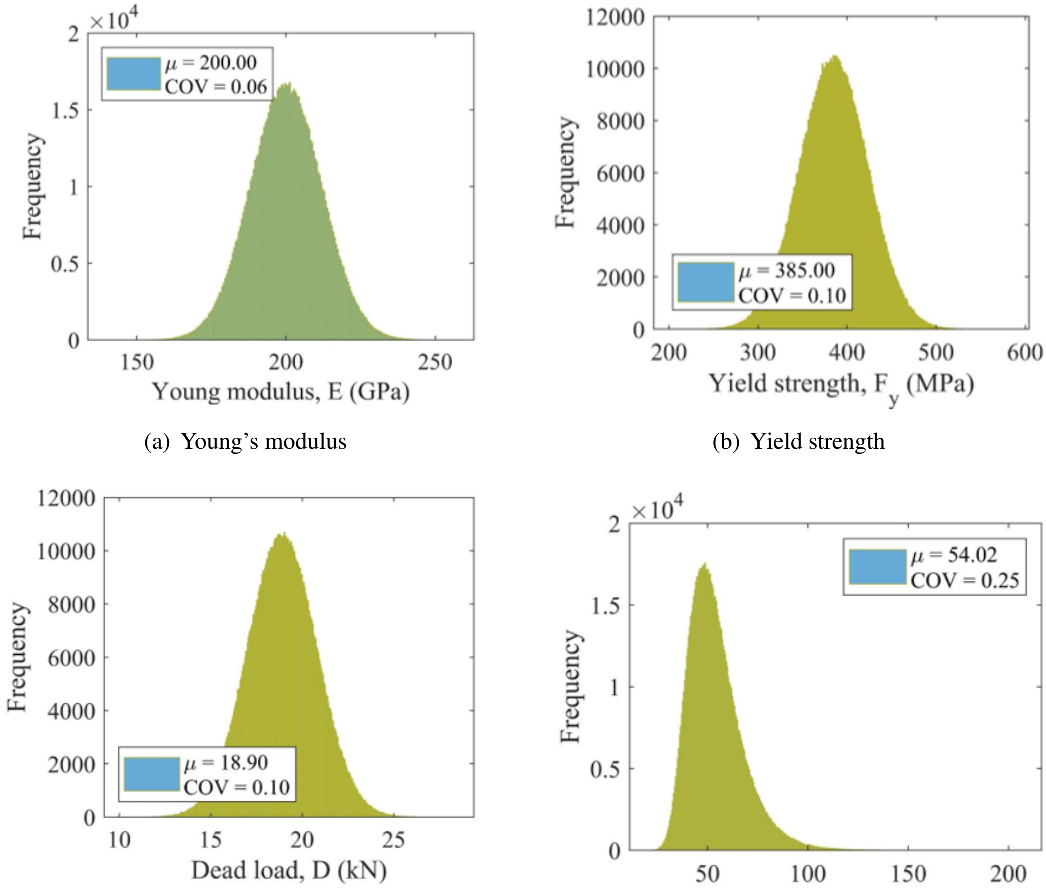

(a) Young's modulus (b) Yield strength

(c) Dead load (d) Live load

Figure 9. Illustrations of several histograms of random variables considered in MCS

In Step 3, *FEM-Truss* program is employed to evaluate the performance functions associated with each sample including all considered variables. The performance functions associated with the critical forces in the tension and compression bars are shown in Eq. (1). In Eq. (1), Q is the axial forces (tension or compression), and R is the corresponding strength of the member of interest. In addition, the performance associated with the maximum deflection of the structure is shown in Eq. (2). The limitation of the deflection, y_{LS} is $L_s/360$ (assuming floor structure), and y is the maximum deflection due to the live load. The routine is repeatedly executed for the entire sampling set generated in Step 4.

$$g = R - Q \tag{1}$$

$$g = y_{LS} - y = \frac{L_s}{360} - y \tag{2}$$

Finally, the probability of failure (P_f) in MCS can be evaluated using Eq. (3). In the equation, N^{fail} is the number of failure events recorded among the N_{MCS} simulations. The reliability index, β

can be converted from P_f using Eq. (4). The statistical information, i.e., the mean, standard deviation, and COV of the performance functions are also determined in this step [3, 24].

$$P_f = \frac{N^{fail}}{N_{MCS}} \tag{3}$$

$$\beta = \Phi^{-1}\left(1 - P_f\right) \tag{4}$$

4. Results and discussions

There are three different feasible sections for tension and two for compression members as selected in Section 2. Noticeably, these sections are designed at the LRFD limit states of interest as discussed in Section 2. This section investigates safety from the probabilistic point of view as presented in Section 3. The tension behaviors are examined for the three feasible sections and reported in Fig. 10. Similarly, the results of the compression bars are captured in Fig. 11 for two chosen sections. It is worth noting that the considered truss is a statistically determinate structure. Therefore, the resultants (i.e., the axial forces Q) are not dependent on the sections designed, whereas the resistances (R) strongly depend on the specific sections designed. Consequently, the statistical properties of Q are observed similarly in Fig. 10 for tension behavior and Fig. 11 for compression cases.

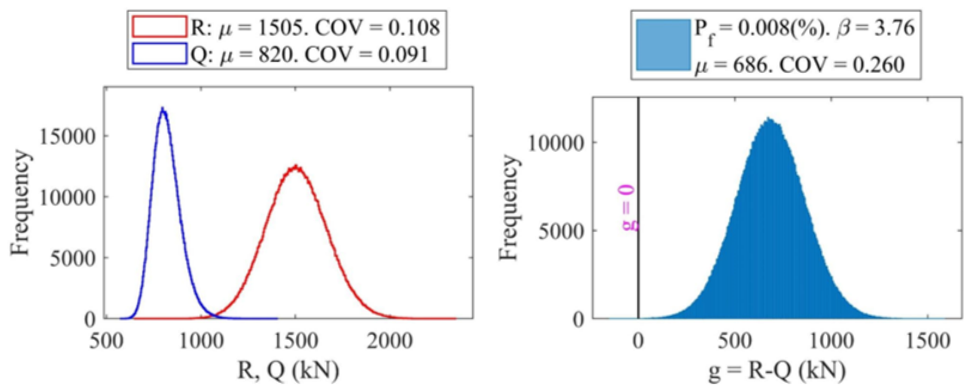

(a) RHS Section of 120 × 120 × 10 mm

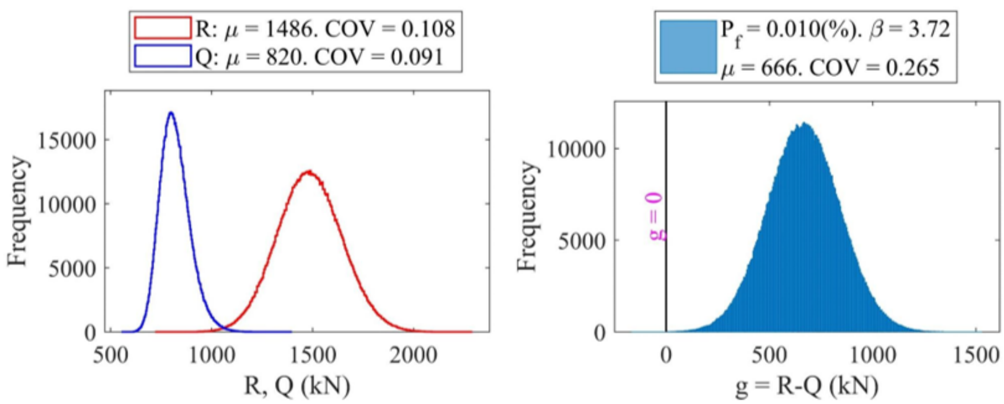

(b) RHS Section of 140 × 140 × 8.0 mm

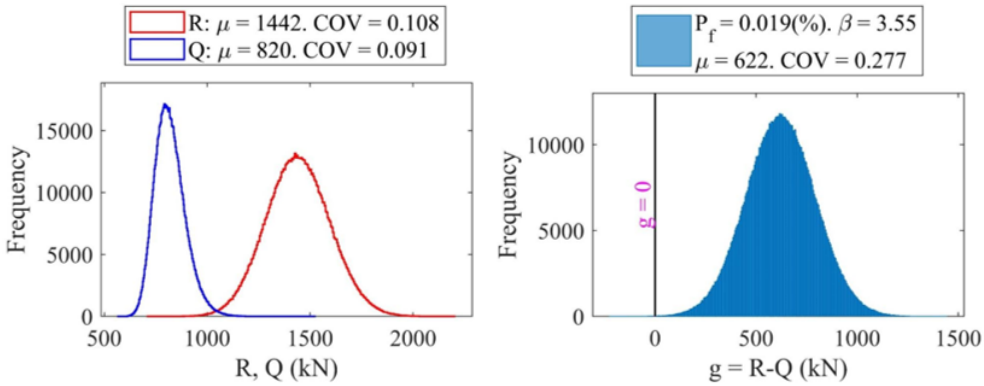

(c) RHS Section of 150 × 150 × 7.1 mm

Figure 10. Results of MCS for tension bar

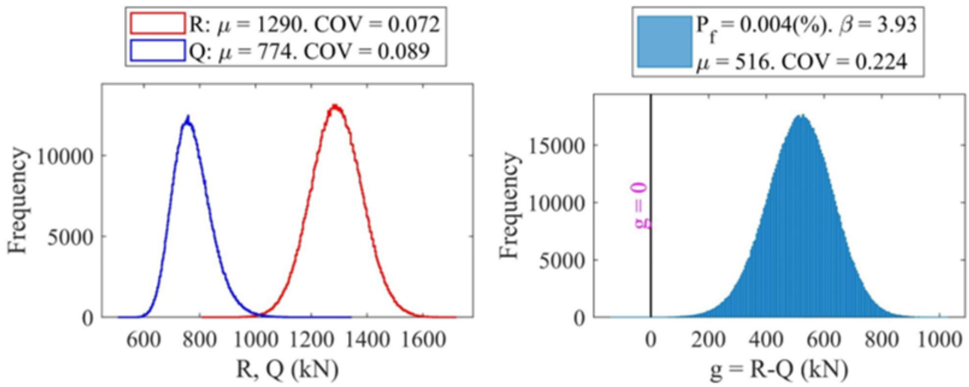

(a) RHS Section of 180 × 180 × 8.8 mm

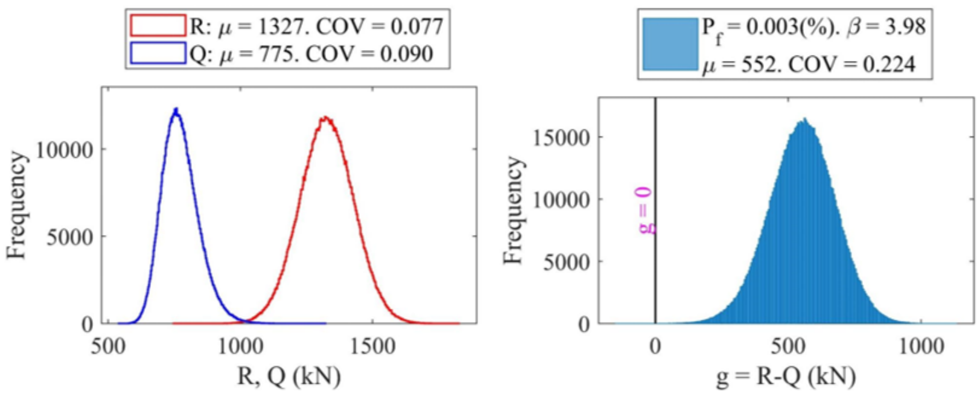

(b) RHS Section of 200 × 200 × 7.1 mm

Figure 11. MCS results for compression bar

It is seen in Fig. 10 and Fig. 11 that all RIs relating to the strength limit states are all higher than the target value of 3.0, which is specified in AISC 360-16 and ASCE/SEI 7-16 [7, 18]. In addition, the RIs for compression members are much higher than the target value. Moreover, the RIs for compression are also higher than those for tension behaviors. Here, it can be stated that the compression behavior is specified with more redundancy in the current codes, although they are designed at the limit states as indicated by the ratio between the P_r and P_u. These observations imply that the resistance factors for tension and compression designs in AISC 360-16 are conservatively specified for truss members. In other words, the resistance factors specified in the current design code can be increased to make the actual RI meet the target value. In this context, the MCS-based framework proposed in this study is recommended for reliability analyses.

The COV terms reflect the uncertainty levels of the variables. The COVs of both load and resistance are summarized in Fig. 10 and Fig. 11 for tension and compression, respectively. It is seen that the COVs of axial loads are the same at about 0.09. However, the COVs of tension resistances are observed higher than those for compression. Thus, the COVs of the performance functions relating to tension are also higher than those for the compression, as depicted in the right panels of Fig. 10 and Fig. 11. As a result, the RIs for the tension are lower than those for compression behaviors. Moreover, the different COVs of the performance function relating to tensions are also captured although the uncertainties in the material are similar for the two behaviors. These observations illustrate that the MCS can reflect the feature of uncertainties more accurately than the point estimate method, which was performed in the development of current design codes.

The comparisons of the design solutions are summarized in Table 2. It is seen that the RIs for each behavior (compression or tension) are relatively identical when the sections are sized at the LRFD limit state (indicated by the unity ratios of P_r and P_u).

Table 2. Comparison of the feasible sections

No.	Behavior	Section (mm)	Weight (kg/m)	P_r/P_u	RI
1	Compression	$180 \times 180 \times 8.8$	45.2	1.00	3.93
2	Compression	$200 \times 200 \times 7.1$	41.6	1.02	3.98
3	Tension	$120 \times 120 \times 10$	40.57	1.05	3.76
4	Tension	$140 \times 140 \times 8$	40.04	1.04	3.72
5	Tension	$150 \times 150 \times 7.1$	38.85	1.01	3.55

Based on the comparison table, the sections are chosen as $200 \times 200 \times 7.1$ mm for compression and $150 \times 150 \times 7.1$ mm for tension members. Although the reliability index of the tension behavior is not the highest, the weights of the selected tension chords are the lowest and this size combination helps to easily connect members in the truss structure.

Next, the deflection of the structure is investigated for the chosen sections. The results of MCS are captured in Fig. 12 assuming the maximum deflection at the middle of the span. The RI of 0.95 is assessed for deflection performance considering floor structures, as shown in Fig. 12(a). This value is much lower than those obtained for strength limits shown in Table 2. The target RI under the serviceability was not specified in AISC 360-16. However, it is observed that the RI under the serviceability (e.g., deflection in this study) is commonly lower than that of the strength limit state [25, 26]. Particularly, the RI regarding the deflection was reported as about zero in the previous study [27]. This is because the consequences of failures concerning the serviceability limit states are minor or moderate in comparison with those relating to the strength limit states [28].

Alternatively, if the truss structure is designed for the roof members, then the limiting deflection of $L_s/240$ needs to be applied as specified in AISC 360-16. In this context, the RI of 3.66 is obtained in the MCS as shown in Fig. 12(b). That means the RI increases about four times when the same structure is used from the floor to the roof member. This observation indicates that the different limiting of deflections will result in very different RIs of floor or roof members in the same building.

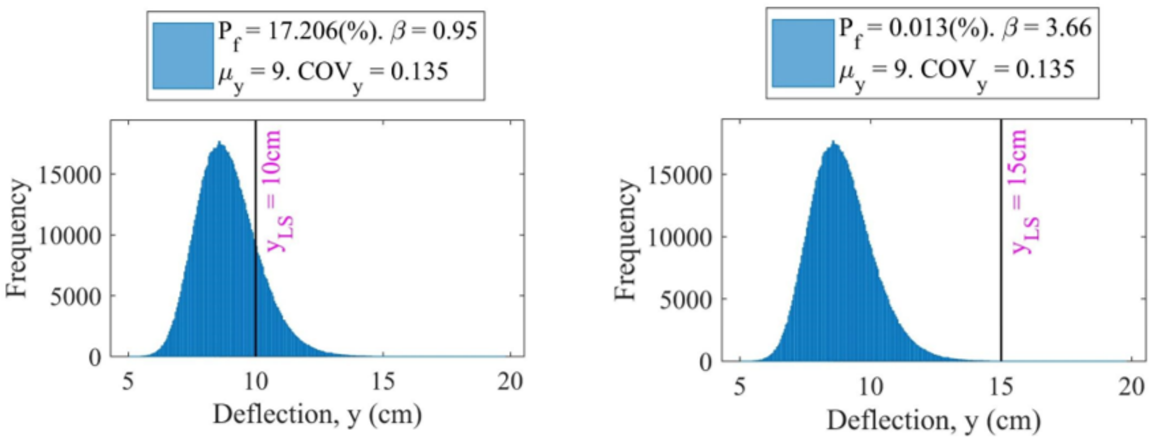

(a) For limiting deflection (y_{LS}) of $L_s/360$

(b) For limiting deflection of $L_s/240$

Figure 12. Results from MCS concerning deflection limit state

5. Conclusions

This study investigates the safety of the truss structure from a probabilistic point of view. The limit states concerning the strength and serviceability are handled. The sections of the truss members are first designed using the LRFD specification. Then, the MCSs are performed to evaluate the failure probabilities and the reliability indexes for the considered performances. Several conclusions are established as follows.

A procedure for applying MCS as additional analyses is presented to elicit insight into the LRFD-based design solutions. The results of the examined truss demonstrate that all of the strength limit states are redundantly satisfied with the target value specified in the current design codes, although the sections are designed at the limit state (depicted by the most likely unity ratio of P_r and P_u).

The excess of safety in terms of RI for both tension and compression bars demonstrates that the resistance factors specified in the current codes are overestimated since they are obtained from the MVFOSM. Thus, if the resistance factors are specifically calibrated for individual problems with the aid of MCS, using them might then provide more uniform design solutions as the main purpose of the reliability-based design codes. Consequently, more economical design solutions will be achieved.

Pertaining to the serviceability limit state, the RI is much lower than those estimated for the strength limit states. Furthermore, the RI for the serviceability limit state (i.e., deflections in this study) strongly depends on the limiting values specified in the design codes. It is also observed that the RI is different about four times when the same structure is applied to the floor or the roof members.

Acknowledgments

This research is funded by Vietnam Maritime University under grant number: DT22-23.73.

References

[1] Ditlevsen, O., Madsen, H. O. (2007). *Structural reliability methods*. Department of Mechanical Engineering Technical University of Denmark: Denmark.

[2] Ang, A. H., Tang, W. H. (1984). *Probability concepts in engineering planning and design, Vol. 2: decision, risk, and reliability*. John Wiley & Sons: New York, USA.

[3] Haldar, A., Mahadevan, S. (2000). *Probability, reliability and statistical methods in engineering design*. John Wiley: Hoboken, NY, USA.

[4] Allen, T. M., Nowak, A. S., Bathurst, R. J. (2005). *Calibration to determine load and resistance factors for geotechnical and structural design*. Transportation Research Circular: Washington, DC, USA.

[5] Nowak, A. S., Collins, K. R. (2000). *Reliability of structures*. McGraw-Hill: New York.

[6] AASHTO (2017). *LRFD Bridge Design Specifications*. AASHTO: Washington, DC, USA.

[7] AISC 360-16 (2016). *Specification for structural steel buildings*. American Institute of Steel Construction: Chicago, USA.

[8] Phoon, K.-K., Ching, J. (2018). *Risk and reliability in geotechnical engineering*. CRC Press: New York, USA.

[9] MLIT (2009). *Technical standard and commentaries for port and harbor facilities in Japan*. Ministry of Land, Infrastructure, Transport and Tourism (MLIT): Ports and Harbors Bureau: Tokyo, Japan.

[10] Doan, N. S., Huh, J., Mac, V. H., Kim, D., Kwak, K. (2020). Probabilistic risk evaluation for overall stability of composite caisson breakwaters in Korea. *Journal of Marine Science and Engineering*, 8(3): 148.

[11] Phoon, K.-K. (2016). Role of reliability calculations in geotechnical design. *Georisk: assessment and management of risk for engineered systems and geohazards*, 11(1):4–21.

[12] Low, B. K., Phoon, K.-K. (2015). Reliability-based design and its complementary role to Eurocode 7 design approach. *Computers and Geotechnics*, 65:30–44.

[13] MATLAB. *MATLAB (2020b)*. The Mathworks Inc., Natick, Massachusetts, USA.

[14] Cook, R. D., Malkus, D. S., Plesha, M. E., Witt, R. J. (2002). *Concepts and applications of finite element analysis*. 4th edition, Willey: New York.

[15] Logan, D. L. (2010). *A first course in the finite element method*. 5th edition.

[16] Blum, H. B. (2013). *Reliability-based design of truss structures by advanced analysis*. Research Report R936, The University of Sydney, Sydney, Australia.

[17] Packer, J. A., Wardenier, J., Zhao, X.-L., van der Vegte, G. J., Kurobane, Y. (2009). *Design guide for rectangular hollow section (RHS) joints under predominantly static loading*. 2nd edition, CIDECT: Germany.

[18] ASCE/SEI 7-16 (2016). *Minimum design loads for buildings and other structures*. American Society of Civil Engineers: Reston VA.

[19] Nowak, A. S., Collins, K. R. (2012). *Reliability of structures*. 2nd edition, CRC Press: Boca Raton, FL, USA.

[20] Doan, N. S., Dang, P. V., Huh, J., Mac, V. H., Haldar, A. (2022). Efficient approach for calibration of load and resistance factors in the limit state design of a breakwater foundation. *Ocean Engineering*, 251: 111170.

[21] Ellingwood, B., Galambos, T. V., MacGregor, J. G., Cornell, C. A. *Development of a Probability Based Load Criterion for American National Standard A58 - Report 577*. 1st edition, National Bureau of Standards: Washington D. C., USA.

[22] Galambos, T. V., Ravindra, M. K. (1981). Load and resistance factor design. *Engineering Journal, AISC*, 18(3):78–84.

[23] Zhang, H., Liu, H., Ellingwood, B. R., Rasmussen, K. J. R. (2018). System reliabilities of planar gravity steel frames designed by the inelastic method in AISC 360-10. *Journal of Structural Engineering*, 144 (3).

[24] Doan, N. S., Huh, J., Mac, V. H., Kim, D. H., Kwak, K. (2021). Calibration of Load and Resistance Factors for Breakwater Foundations under the Earthquake Loading. *Sustainability*, 13(4):1730.

[25] CAN/CSAS614:2014 (2014). *Canadian highway bridge design code*. Canadian Standards Organization: Mississauga, Ontario, Canada.

[26] Galambos, T. V., Ellingwood, B. (2013). Serviceability limit states. In *Design of Steel-Concrete Composite Bridges to Eurocodes*, CRC Press, 442–465.

[27] Ghasemi, S. H. (2015). Target reliability analysis for structures. PhD thesis, Graduate Faculty of Auburn University.

[28] Bhattacharya, B., Basu, R., tung Ma, K. (2001). Developing target reliability for novel structures: the case of the Mobile Offshore Base. *Marine Structures*, 14(1-2):37–58.